Journal of Thermal Analysis, Vol. 54 (1998) 707-719

REVERSIBLE MELTING OF THERMALLY FRACTIONATED POLYETHYLENE

F. Cser[1], *J. L. Hopewell*[1] *and R. A. Shanks*[2]

[1]CRC for Polymers, 32 Business Park Dr., Notting Hill, 3168
[2]Applied Chemistry, RMIT University, Melbourne, 3000, Australia

(Received May 5, 1998)

Abstract

Different grades of linear low density polyethylenes (LLDPEs) have been quenched cooled step-wise and crystallised isothermally at (a series of increasing) temperatures in a DSC (thermal fractionated samples). These samples have been investigated by temperature modulated DSC (MDSC). The heat flow curves of the thermal fractionated materials were compared with those obtained from samples crystallised at a relatively slow cooling rate of 2 K min^{-1} (standard samples).

The melting enthalpy obtained from the total heat flow of the thermal fractionated samples was 0–10 J g^{-1} higher than those of standard samples. The melting enthalpy obtained from the reversing heat flows was 13–31 J g^{-1} lower in the thermal fractionated samples than in the standard samples. The ratio of the reversing melting enthalpy to the total melting enthalpy increased with decreasing density of the PE. The melting temperature of the endotherms formed by the step-wise cooling was 9 K higher than the crystallisation temperature.

Keywords: polyethylene, reversible melting, thermal fractionation, TMDSC

Introduction

We showed in our previous papers [1–4] that some reversibility in the melting of semicrystalline polymers is always present. It is a relaxation motivated process as its extent in the melting process depends on the modulation frequency. It also depends on the chemical structure of the polymer, i. e. the more branched the polymer the greater the reversibility of the melting [2]. It has also been shown that the heat capacity and hence the reversing heat flow, decreases rapidly during the annealing the polymers within their melting range [3–4]. The change in the heat capacities is fast, generally it is completed within a few minutes (<3 min).

Varga *et al.* [5] studied the stepwise crystallisation of low density polyethylene (LDPE). They found that LDPE cooled in a DSC instrument with stepwise crystallisation showed a multiple endotherm melting process. They called the phenomenon a 'melting memory effect' of the polymer. It could be completely eliminated by heating the sample above its melting temperature or stretching it to

1418–2874/98/ $ 5.00

Akadémiai Kiadó, Budapest
Kluwer Academic Publishers, Dordrecht

above 410%. Nevertheless, the individual crystals with different melting temperatures were stable and they could be eliminated gradually, starting from those of the lowest melting temperature, by increased strain.

Multiple melting endotherms could also be produced with polypropylene (PP) using a reversed annealing technique. This means, the crystallised sample has been heated below the melting temperature, kept there for a time, then cooled to crystallise isothermally at different decreasing temperatures in the consecutive cycles between 100 and 130°C for a time. The sample is heated again to another temperature lower than that of the previous cycle, annealed, then cooled to crystallise isothermally and so forth [6–7]. The crystallisation temperature was selected high enough to prevent the β to α transition. The resultant heat flow curve recorded by a melting scan in the DSC showed a multiple endotherm melting of β-PP. The authors concluded [5] that the individual melting endotherms result from crystals with different lamellar thickness and/or perfection originating from the 'polymolecularity according to the chemical structure'.

As the same process did not result in multiple endotherms in the melting process of PP the phenomenon found for LDPE can be attributed to a fractionation-like process, where the crystals with different melting endotherms might contain macromolecules with different branching density [8–10]. Hence the thermal memory effect can be regarded as a form of a fractionation, i.e. thermal fractionation (TF).

In other papers [11, 12] it has been shown DSC results obtained on thermally fractionated LLDPE, high density polyethylene (HDPE) and very low density polyethylene (VLDPE). We have found that branching is essential to obtain TF of the material. We have found that a lamellar thickness calculated on the basis of the melting temperature correlated with the lamellar thickness of the crystals determined from the Guinier plot of small angle X-ray scattering (SAX) intensities [12].

The aim of this study is to check the thermal fractionation hypothesis by using MDSC to study the effect of the TF on the response of different polymeric materials. This paper is dealing with the reversing/non-reversing response of different LLDPEs and HDPE to the stepwise cooling.

Experimental

Materials

C8-LLDPE1: Solution polymerised with octene comonomer, ρ=923 kg m^{-3}, MFI: 0. 94 g $(10\ min)^{-1}$.

C8-LLDPE2: Solution polymerised with octene comonomer, ρ=923 kg m^{-3}, MFI: 1.10 g $(10\ min)^{-1}$.

C6-LLDPE: Gas phase polymerised with hexene comonomer, ρ=922 kg m^{-3}, MFI: 0.78 g $(10\ min)^{-1}$.

C4-LLDPE: Gas phase polymerised with butene comonomer, ρ=918 kg m^{-3}, MFI: 1.00 g $(10\ min)^{-1}$.

Me-LLDPE: Polymerised by metallocene catalyst with butene comonomer, ρ=910 kg m^{-3}, MFI = 1.2 g (10 min)$^{-1}$.
HDPE: extrusion grade polymer, MFI: 0.2 g (10 min)$^{-1}$.

Sample preparation

6–9 mg flat samples were placed in sample pans of the temperature modulated DSC (MDSC). Two samples of the same kind were placed in a Perkin-Elmer DSC-7. The samples were heated 20 K above their melting temperature and than cooled at 200 K min^{-1} to the starting temperature of isothermal crystallisation given in Table 1. After a 100 min crystallisation time the samples were stepwise annealed by decreasing temperatures steps of 4 K. The samples were held at each crystallisation temperatures for 100 min. Six or seven additional steps were used. The thermal programs were different for the different types of PE (Table 1).

Table 1 Temperature programs for the step-wise crystallisation of LLDPE samples in °C

Step #	1	2	3	4	5	6	7	8
LLDPE	122	118	114	110	106	102	98	94
Metallocene	94	90	86	82	78	74	70	–
HDPE	136	132	128	124	120	116	112	108

MDSC testing

A TA Instrument MDSC is used for the study. An intercooler cell was operated using nitrogen as the heat transformer gas with a flow rate of 100 mL min^{-1}. Helium with a flow rate of 25 mL min^{-1} was used as a purge gas. The modulation period was 40 sec and modulation amplitude was 0.6 K. This is a heating and cooling form of modulation [1].

One of the pair of samples was analysed by two consecutive heating and cooling cycles using 2 K min^{-1} heating and cooling rates. The first heating/cooling cycle showed the properties of the TF state, the second cycle showed that of the standard (ST) state. The data are shown in this paper. The second was treated by reversed annealing. The data obtained by this latter experiment will be published elsewhere [13].

Data analysis

Transition enthalpies were calculated from the corresponding heat flow curves (total, reversing and kinetic) and are given in Table 2. The upper limit of the integration limits was the end of the melting endotherm. The lower limit of the integration was obtained from the heat capacity curves according to [2, 4].

This means the temperature, when the heat capacity was recorded upon cooling, approached the heat capacity recorded upon heating. This was 10–40°C for the different LLDPEs and 90°C for HDPE. Details of the method are given in our previous papers [1–4].

Heat flows obtained on TF samples have also been compared with those of the ST. The former curves have been subtracted from the latter ones and these difference curves have been integrated from 10 to 130°C.

Results and discussion

Figure 1 shows the heat capacity of C8-LLDPE1. Both the heating and cooling cycles are shown.

The heat capacity curves are identical below the temperature range of the transition, i.e. below 40 °C. Above this temperature the heating curves show an increase during the TF cycle heat capacity values with respect to the ST values up

Table 2 Melting enthalpies of the different materials integrated from the total, the reversing and the kinetic heat flows respectively, all in [J g^{-1}]

	C8-LLDPE1	C8-LLDPE2	C6-LLDPE	C4-LLDPE	Me-LLDPE	HDPE
			1st heating cycle			
Total	123.2	137.9	141.4	116.0	91.5	177.5
Reversing	98.5	107.8	106.5	75.0	39.1	85.0
Kinetic	24.7	29.84	34.74	42.7	52.3	98.5
Kinetic (peak)	39.0	45.1	50.9	–	–	–
			1st cooling cycle			
Total	–126.7	–136.0	–143.0	–120.8	–80.3	–177.0
Reversing	–29.4	–39.4	–34.5	–27.1	–15.7	–32.5
Kinetic	–97.3	–96.6	–108.6	–94.0	–64.7	–142.0
			2nd heating cycle			
Total	119.1	132.1	132.9	112.0	80.6	176.0
Reversing	117.6	126.0	122.4	85.2	51.4	99.7
Kinetic	1.5	6.0	10.8	26.5	29.3	74.8
Kinetic (peak)	13.4	11.1	24.8	–	–	–
			2nd cooling cycle			
Total	–127.3	–136.6	–143.7	–122.4	–80.0	–174.6
Reversing	–30.0	–39.1	–34.2	–28.0	–15.9	34.0
Kinetic	–97.6	–97.4	–109.5	–93.6	–64.1	–140.9

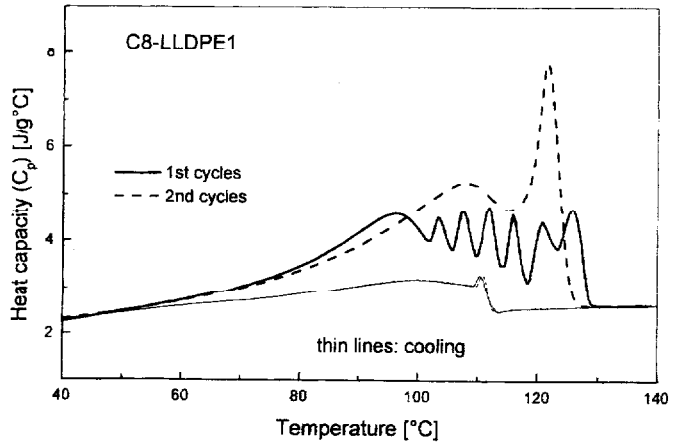

Fig. 1 Heat capacities of a C8-LLDPE1, after thermal fractionation

to approximately 100°C. They decrease after a broad endotherm and oscillate below the values of the ST state forming 6 endotherms up to the melting temperature. The endotherms have a rather sinusoid shape than what would be expected of the sum of Gaussian endotherm peaks. The final endotherm decreased to the heat capacity value of the molten state above the normal melting temperature. There was no influence of the TF on the heat capacities on cooling. The two cooling cycles resulted in identical curves.

Figure 2 shows the total and the kinetic heat flows of C8 LLDPE1. The kinetic heat flow curve on cooling was practically identical to those of the total heat flows, therefore only the curves measured on heating are given.

The total heat flow curves are identical in the first and the second cycle up to 90°C. Their values are then slightly higher in the TF cycle than in the ST cycle.

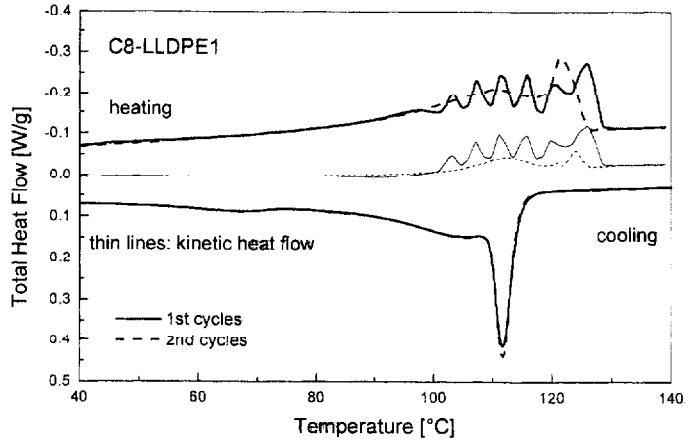

Fig. 2 Heat flow curves of a C8-LLDPE1, after thermal fractionation

After a broad endotherm an oscillation starts – as in the heat capacity curves – but this oscillation was around the total heat flow curve of the second run, i.e. the standard state. There was also 6 melting endotherms in the heat flow curves of the first heating cycle. The form of the melting endotherms was neither Gaussian nor Lorentzian, therefore the total heat flow curves could not be deconvoluted into individual endotherms. The first curve of total heat flow was a quasi-sinusoidal superposition on the second curve in the melting range, with the exception of the last two endotherms, which had smaller values than the single strong endotherm in the standard state. The starting temperature of the stepwise crystallisation (122°C) was above the crystallisation temperature obtained by slow (2 K min^{-1}) cooling, i.e. 120°C. Therefore the first step did not form crystals in the system.

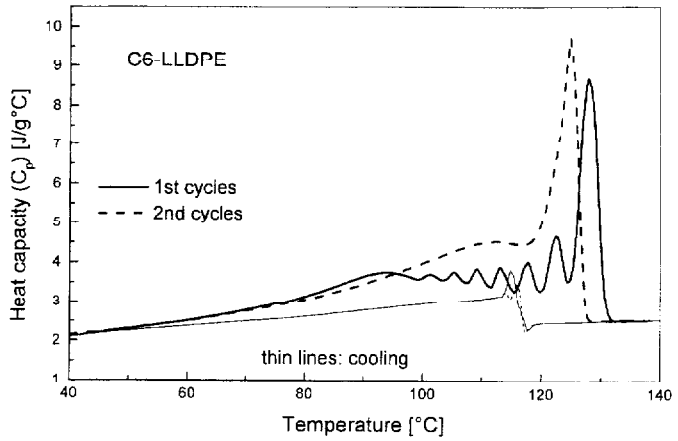

Fig. 3 Heat capacities of a C6-LLDPE, after thermal fractionation

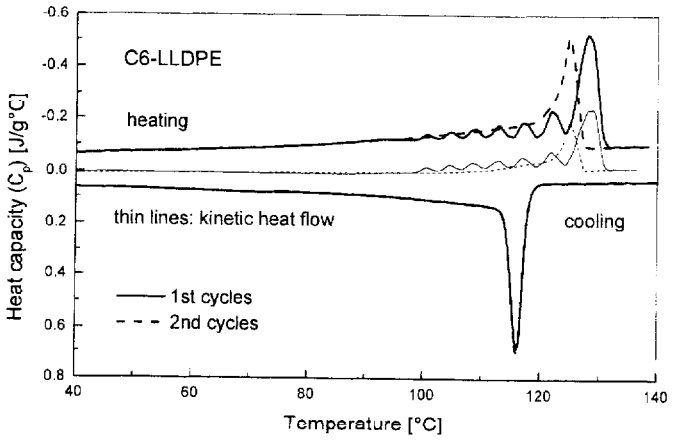

Fig. 4 Heat flow curves of a C6-LLDPE, after thermal fractionation

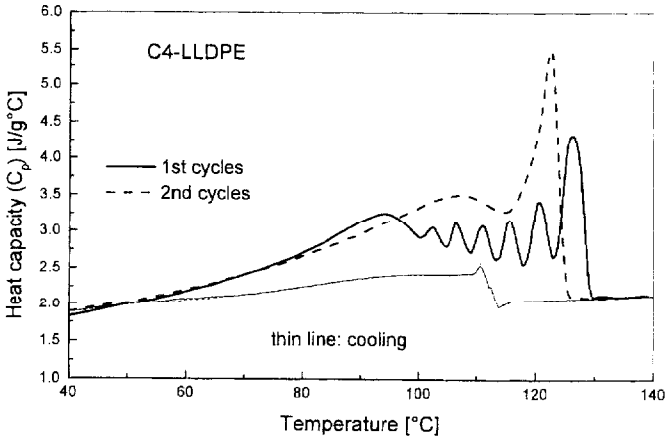

Fig. 5 Heat capacities of a C4-LLDPE, after thermal fractionation

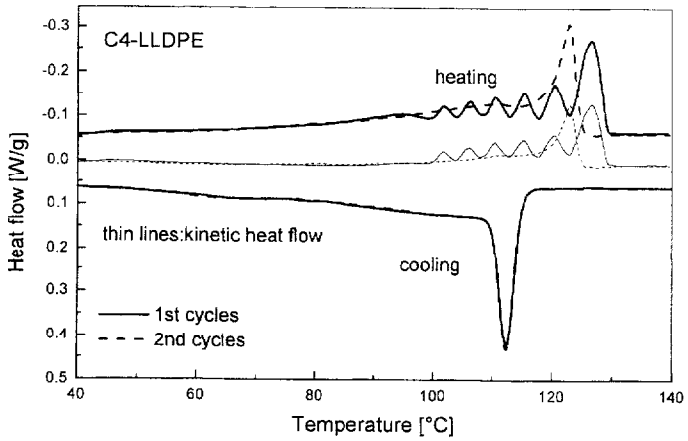

Fig. 6 Heat flow curves of a C4-LLDPE, after thermal fractionation

The kinetic heat flow was zero up to 70°C. Then there was a small decrease followed by six endotherms, each one being above the kinetic heat flow value of the ST cycle.

The melting enthalpies integrated from the heat flow curves from 10°C were collected in Table 2. The melting enthalpy obtained from the total heat flow was practically the same in both cycles. There was a small increase in the degree of crystallinity in the TF state with respect to the ST one. The melting enthalpy of the reversing component was much lower in the TF state and that of the kinetic component was higher with respect to the ST state.

Table 2 contains the transition enthalpies of C8-LLDPE2 as well. Its curves are not shown here as they are very similar to C8-LLDPE1 shown in this paper.

Its crystallinity is higher than that of C8-LLDPE1. The differences in their monomer content – and consequently in their densities – did not influence their behaviour in the TF experiment.

Figures 3 and 4 show the heat capacity and the heat flow curves for C6-LLDPE. The same features described for the previous materials can be observed here. But the magnitude of the influence is smaller. A strong melting endotherm dominates the heat flow curves and the amplitude of the oscillation is smaller here than for the previous example. The melting enthalpies change similarly to those of the previous material. The integrated transition enthalpies are also collected in Table 2. The transition enthalpies show here the greatest crystallinity and increase in the melting enthalpies in TF state with respect to the ST state. Nevertheless, this difference is small (<10 J g^{-1}).

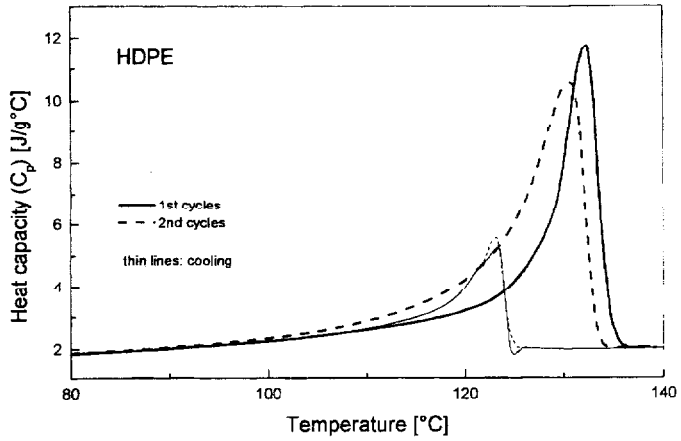

Fig. 7 Heat capacities of HDPE, after thermal fractionation

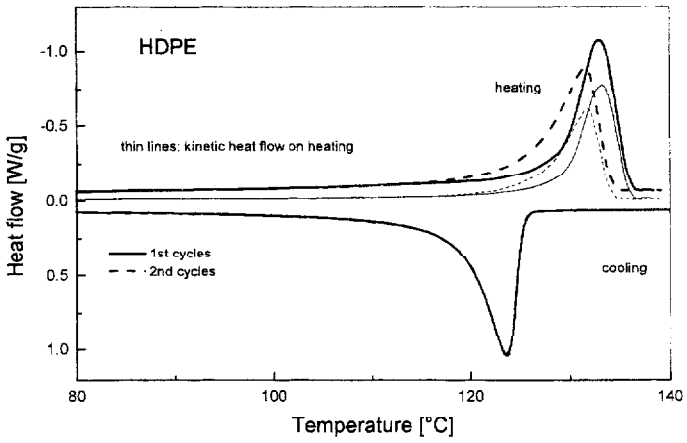

Fig. 8 Heat flow curves of HDPE, after thermal fractionation

C4-LLDPE behaves analogously to the C8-LLDPE1 as seen in Figs 5 and 6. The transition enthalpies are given in Table 2. This is the least crystalline of the LLDPEs studied.

Figures 7 and 8 show the result of a TF experiment for HDPE giving the heat capacity and heat flow curves. There are no additional endotherms on the curves. The melting endotherm appears at a higher temperature on the TF sample than on the ST sample. HDPE has the smallest increase in the transition enthalpies of the TF state with respect to the ST state. The curve integrated from the reversing heat flow formed the smallest extent of melting enthalpy with respect to the total heat flow.

As HDPE did not show multiple endotherms in the melting after a similar crystallisation process, the results seemingly support the concept that thermal fractionation is occurring. We tried to support the concept by another experi-

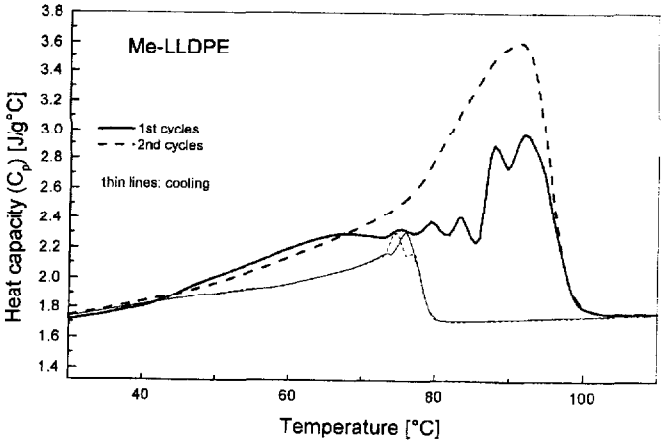

Fig. 9 Heat capacities of a Me-LLDPE, after thermal fractionation

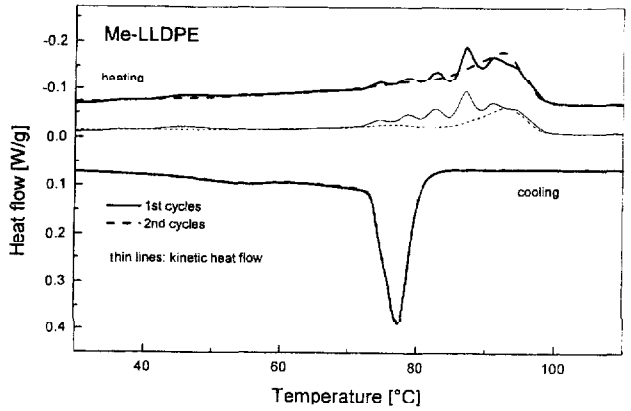

Fig. 10 Heat flow curves of a Me-LLDPE, after thermal fractionation

ment, i. e. recording the heat flow and heat capacity curves of a LLDPE produced using metallocene catalyst. This polymer should not show great differences in the distribution of the branching and in the molar mass [14], although, recently Hsieh and coworkers [15] challenged this conception. Therefore we expected its response to be analogous to that of HDPE but with a lower melting temperature.

As the crystallisation temperature of Me-LLDPE was only 90°C, the TF program was started at 94°C (Table 1). Figures 9 and 10 show the heat capacity and heat flow curves for the LLDPE produced using metallocene catalyst.

There are 5 endotherms in all of the TF experiment thermal responses shown in Figs 9 and 10. Additionally, a shoulder was also present on the final en-

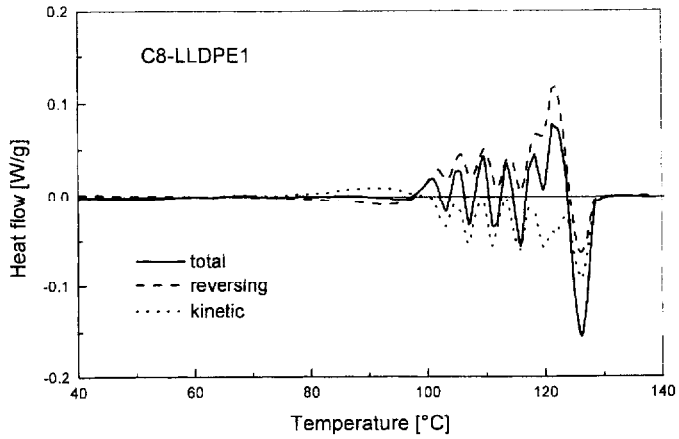

Fig. 11 Difference between the first and second heating cycle of a C8-LLDPE1, after thermal fractionation

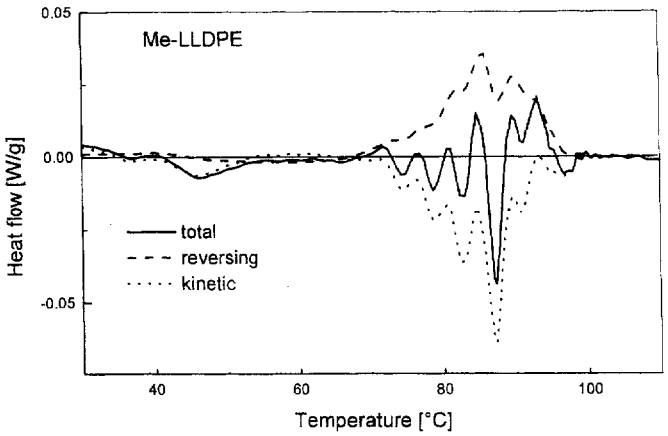

Fig. 12 Difference between the first and second heating cycle of a Me-LLDPE, after thermal fractionation

dotherm. The amplitude of the oscillation was smaller here than for the other LLDPEs studied.

A comparison of the total, reversing and kinetic heat flow curves of all of the studied materials has been carried out. The results for only two of the polymers are shown here. Figure 11 shows the difference between the curves for the first and the second heating cycles for the total, the reversing and the kinetic heat flows for C8-LLDPE1, Fig. 12 shows comparable data for Me-LLDPE.

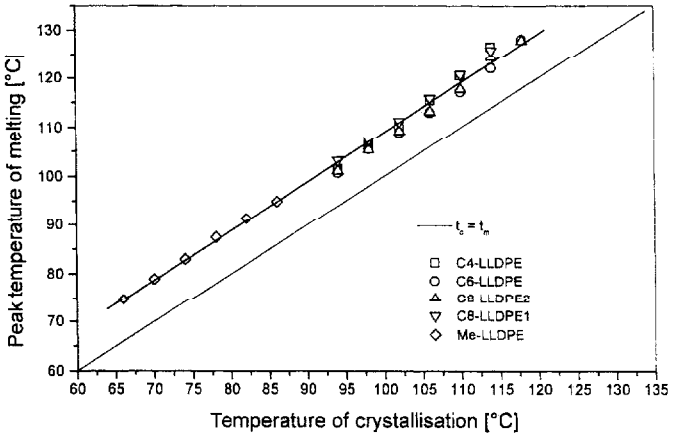

Fig. 13 Endotherm melting temperature *vs.* crystallization temperature of different LLDPE-s, after thermal fractionation

There is practically no difference in the heat flow curves below 70°C for LLDPE produced by non-metallocene catalyst. The total heat flow curve then oscillated around the zero line. The integral of the difference curves are summarised in Table 3. It is nearly zero for the total heat flows of all of the studied samples. It is a negative value for the reversing heat flows. This means, that the reversibility of the transition is decreased by the long times of annealing during the crystallisation. Nevertheless, the reversing heat flow does not disappear after the TF process. It dominates all of the melting of the Me-LLDPE.

For HDPE the thermal fractionation techniques did not resulte in multiple endotherms. Nevertheless there was a decrease in the melting enthalpy integrated

Table 3 Integrals of the difference curves of the first and second heating cycles after thermal fractionation in [J g^{-1}]

	C8-LLDPE1	C8-LLDPE2	C6-LLDPE	C4-LLDPE	Me-LLDPE	HDPE
Total	−7.2	0.3	4.07	−3.0	−3.0	9.8
Reversing	−22.3	−31.4	18.1	12.9	12.9	−17.9
Kinetic	29.6	31.8	22.2	7.45	10.2	27.5

from the reversing heat flow and there is an increase in the melting temperature (2 K)

The data shown above do not completely confirm the concept of thermal fractionation. There are multiple endotherms given by the LLDPE sample prepared by metallocene catalyst where, according to the reports [14], the distribution of the branching is homogeneous. This does not support thermal fractionation. This means, either the LLDPEs produced using metallocene catalyst (or this particular material) do not have uniform branching, as stated in [15], or the melting memory effect, cannot be treated as a true thermal fractionation. Nevertheless, the experiments showed that the presence of branching seems to be crucial for the phenomenon.

The crystallisation temperature of the individual endotherms can be determined starting from the lowest step. The response to the first crystallisation step at the highest temperature is not seen on the curves. The peak endotherm temperatures of the individual endotherms are represented as a function of the crystallisation temperatures in Fig. 13. They form straight lines that do not approach the equal temperature line at increasing temperature. They form straight lines that are parallel to the $T_c=T_m$ line. This means, an equilibrium melting temperature of the material, which is characteristic of the average length of the unbranched chain segments, cannot be calculated in this way [16].

Conclusions

The step-wise cooling and annealing for 100 min did not produce equilibrium crystals. The maximum temperatures of the individual endotherms follow merely the temperature of the crystallisation by a constant shift of 8.9°C. The fluctuation of the heat flow curve around its standard state is not a result of a superposition of several individual melting endotherms. The annealing of the crystals which have already been formed at the temperature of the crystallisation transfers the melting of crystals from a lower melting temperature range to a higher one. This transfer results in a lower reversing and a higher kinetic fraction of the total heat flow in the melting range. Further studies will be carried out to provide a proper explanation for the multiple melting endotherm.

References

1 F. Cser, F. Rasoul and E. Kosior, J. Thermal Anal., 50 (1997) 727.
2 F. Cser, F. Rasoul and E. Kosior, J. Therm. Anal. Cal., 52 (1998) 293.
3 F. Cser, J. Hopewell and E. Kosior, J. Therm. Anal. Cal., 53 (1998) 493.
4 F. Cser and R. A. Shanks, J. Therm. Anal., 54 (1998) 637.
5 J. Varga, J. Menczel and A. Solti, J. Thermal Anal., 17 (1979) 333.
6 J. Varga, J. Thermal Anal., 31 (1986) 165.
7 J. Varga and E. Toth, Macromol. Chem. Macromol. Symp., 5 (1986) 213.

8 A. Peterlin: J. Mater. Sci., 6 (1971) 490.
9 C. J Neves., E. Monteiro and A. C. Habert, J. Appl. Polym. Sci., 50 (1995) 817.
10 E. Adisson, M. Ribeiro, A. Deffieux and M. Fontanille, Polymer, 33 (1992) 4337.
11 R. A. Shanks, K. Tajne and F. Cser, poster paper, Macro'98, Gold Coast, Queensland, Australia (1998).
12 R. A. Shanks and F. Cser: poster paper, Macro'98 Gold Coast, Queensland, Australia (1998).
13 F. Cser, J. L. Hopewell, K. Tajne and R. A. Shanks, J. Therm. Anal. Cal., (to be published) (1998).
14 F. Garbassi, L. Gila and A. Proto, Polymer News, 19 (1994) 367.
15 E. T. Hsieh, C. C. Tso, J. D. Byers and T. W. Johnson, J. Macromol. Sci. - Phys., B36 (1997) 615.
16 B. Wunderlich, Macromolecular Physics, Academic Press, NY 1976.